Vegetable Research

ARTICLE

Open Access

https://doi.org/10.48130/vegres-0026-0015

Vegetable Research **2026**, 6: e025

Genome-wide identification of the *DMP* gene family and CRISPR/Cas9-mediated editing of the *DMP9* gene in radish (*Raphanus sativus* L.)

Peng Zhang[1#], Boya Zhao[1#], Hongxiang Dong[1#], Maoyi Wang[1], Xiaoli Zhang[1], Jiali Ying[1], Feng Cui[2], Sen Chen[1], Jingxue Li[1], Liang Xu[1], Yan Wang[1] and Liwang Liu[1*]

[1] *National Key Laboratory of Crop Genetics & Germplasm Enhancement and Utilization, Key Laboratory of Horticultural Crop Biology and Genetic Improvement (East China) of MOAR, College of Horticulture, Zhongshan Biological Breeding Laboratory, Nanjing Agricultural University, Nanjing 210095, China*

[2] *College of Horticulture and Landscape Architecture, Yangzhou University, Yangzhou 225009, China*

[#] Authors contributed equally: Peng Zhang, Boya Zhao, Hongxiang Dong

[*] Correspondence: nauliulw@njau.edu.cn (Liu L)

Abstract

The *DMP* (Domain of Unknown Function 679 Membrane Proteins) gene family consists of proteins specifically expressed in plant membranes with functions associated with gamete fusion. However, its functional characterization remains largely unexplored in radishes (*Raphanus sativus* L.). In this study, a total of 13 *DMP* genes were identified in the radish genome; they were distributed unevenly across six chromosomes. Phylogenetic analysis revealed five distinct clades, based on the classification and nomenclature of this gene family in *Arabidopsis*. *RsDMP9* was grouped with the haploid-inducing genes *AtDMP8* and *AtDMP9*, which play a potential role in haploid induction. Light, growth, hormone, and stress-responsive elements were identified in the promoter of *RsDMP9*. Quantitative real-time polymerase chain reaction demonstrated the preferential expression of *RsDMP9* in pollen, while other *RsDMP* genes showed differential expression in the roots, petals, and sepals. The RsDMP9 protein was confirmed to be localized to the plasma membrane. The identification and cloning of endogenous U6 promoter sequences from the radish genome were achieved based on the conserved U6 small nuclear RNA (snRNA) sequences of *Arabidopsis thaliana*. *In vivo* imaging and a dual-luciferase reporter system indicated that RsU6-6 exhibited strong transcriptional activity comparable to that of AtU6-1; truncation of RsU6-6 to 326 base pairs could enhance transcriptional activity, making it ideal for single guide RNA (sgRNA) expression and multiplex editing by avoiding promoter crosstalk. Additionally, the CRISPR/Cas9 system driven by RsU6-6 has been shown to achieve a high mutation frequency by protoplast transformation technology, thus demonstrating the effective validation of the CRISPR/Cas9 editing vector in radish protoplasts. These findings provide insights into the evolutionary conservation and functional diversification of *RsDMP* genes, and this protoplast-based editing system would facilitate effectively validating gene function and precision improvement of important traits in radish breeding programs.

Keywords: Radish, *DMP* gene family, *RsDMP9*, Gene editing, U6 promoter

Citation: Zhang P, Zhao B, Dong H, Wang M, Zhang X, et al. 2026. Genome-wide identification of the *DMP* gene family and CRISPR/Cas9-mediated editing of the *DMP9* gene in radish (*Raphanus sativus* L.). *Vegetable Research* 6: e025 https://doi.org/10.48130/vegres-0026-0015

Introduction

Radish (*Raphanus sativus* L.) is an important root vegetable crop belonging to the Brassicaceae family. Radish taproots possess significant nutritional value and health benefits, including antioxidant properties and essential nutrients[1]. As a typical cross-pollinated crop, the high genetic diversity and heterozygosity of the radish present major challenges within populations. This variability complicates consistent selection for desirable traits, necessitating multiple generations of stabilization[2]. Traditional breeding strategies are time-consuming and difficult to purify.

Double Haploid (DH) technology has been widely applied in plant biotechnology due to its advantages in terms of speed and high purity compared to traditional high-generation self-pollination[3,4]. In recent years, the exploration of haploid induction (HI) genes has greatly promoted the development of crop breeding technology. For example, *in vivo* HI technology has been widely applied in maize breeding[5]. The loss-of-function of the PATATIN-LIKE PHOSPHOLIPASE A1/MATRILINEAL/NOT LIKE DAD gene (*ZmPLA1/MTL/NLD*), encoding a phospholipase expressed in sperm, can trigger HI[5–7]. The function of CENTROMERIC HISTONE 3 (*CENH3*) has also been utilized in HI in maize, *Arabidopsis thaliana*, and other plant species[8,9]. Therefore, the combination of gene editing and DH technology provides a potentially efficient way for the rapid improvement of specific traits in breeding programs[10].

The DOMAIN OF UNKNOWN FUNCTION 679 membrane protein (DMP) family constitutes a distinctive group of membrane proteins exclusive to plants, particularly abundant in angiosperms[11,12]. In *Arabidopsis*, the *DMP* gene family comprises ten members, which are distributed across four chromosomes[12]. Among these, *AtDMP1* has been notably implicated in senescence, as it is upregulated during senescence processes in various plant tissues[13]. Furthermore, *AtDMP1* is highly expressed in the dehiscence and abscission zones of siliques. Similarly, *AtDMP3* and *AtDMP4* exhibit upregulation during senescence in rosette leaves, cauline leaves, and siliques[14]. This suggests potential functional overlap in senescence-related pathways[15]. The *AtDMP8* and *AtDMP9* genes encode proteins that localize to the sperm membrane and participate in regulating the sperm–egg fusion process[16]. It has been reported that *ZmDMP* originates from the HI locus *qhir8* in maize[17], and HI was achieved through targeted knockout of *ZmDMP*. Its orthologs, *AtDMP8* and *AtDMP9*, have similarly been successfully identified in *A. thaliana*[10]. In recent years, several orthologs of *AtDMP8* and *AtDMP9* have been functionally validated in monocots (maize,

https://doi.org/10.48130/vegres-0026-0015

rice, etc.) and dicots (*Arabidopsis*, *Brassica napus*, tomato, watermelon, potato, cucumber, etc.), and their knockouts could induce haploids[10,17–22]. However, the characterization and potential roles of the *DMP* family in radish remain elusive, which has significantly hindered progress in haploid breeding and new cultivar development.

The CRISPR (clustered regularly interspaced short palindromic repeats)/Cas9 system is composed of two components: CRISPR-associated protein 9 (Cas9) and a single short guide RNA (sgRNA). It identifies a specific site through complementarity between the sgRNA and the target DNA sequence, enabling genome editing in many species[23]. U6 small nuclear RNA (snRNA) promoters, such as RNA polymerase III (Pol III), play a central role in CRISPR/Cas9 systems by driving the efficient and precise expression of single-guide RNAs (sgRNAs)[23]. The transcriptional activity of U6 promoters directly influences sgRNA expression levels, thereby determining genome editing efficiency[24]. However, these promoters typically exhibit species specificity, resulting in minimal or negligible transcriptional activity in distantly related species. Using species-specific endogenous U6 promoters has been shown to significantly improve gene editing efficiency in species such as cotton[25], apple[26], and strawberry[27]. Nevertheless, the endogenous U6 promoter of the radish has not been reported to date, so there is a lack of crucial components for efficient gene editing in radish.

A genome editing system based on protoplast transient expression has been employed to rapidly assess the editing efficiency of CRISPR constructs and to regenerate transgene-free, gene-edited plants, as demonstrated in citrus[28]. This approach utilizes enzymes to digest leaf or cotyledon tissues and break down cell walls. This procedure yields protoplasts that can be transfected with exogenous nucleic acids, such as CRISPR/Cas9 ribonucleoprotein complexes (RNPs), sgRNAs, or expression vectors, via polyethylene glycol (PEG)-mediated delivery, electroporation, or liposome transfection[29]. Unlike stable transformation, protoplast-based editing enables rapid detection of gene expression or editing efficiency within 24–72 h, eliminating the need for whole-plant regeneration. For regeneration-recalcitrant species like the radish, testing gene editing efficiency through stable transformation is extremely time-consuming. Moreover, while the CRISPR/Cas9 system has revolutionized plant genetic engineering, its utilization in radish remains in a nascent stage. Conversely, protoplast-based transient CRISPR editing provides a platform to quickly evaluate sgRNA targeting efficiency and Cas9 activity without requiring plant regeneration. Therefore, it is imperative to develop a practical and efficient genome editing method for radish that utilizes protoplast transient gene expression.

The objective of this study was to characterize *RsDMP* genes and to screen HI candidates. The evolutionary relationships, structural features, and expression profiles of *RsDMP* genes were also investigated. *RsDMP9*, an ortholog of the haploid-inducing *AtDMP8* and *AtDMP9*, was validated as a key candidate due to its high pollen-specific expression and plasma membrane localization. The isolation and prioritization of the endogenous RsU6-6 promoter (a 326-base pair [bp] truncated variant), together with the establishment of a rapid protoplast-based transient editing platform integrating RsU6-6-driven CRISPR/Cas9, were achieved for gene function validation. These findings offer insights into the evolutionary conservation and functional diversification of *RsDMP* genes, address gene-editing challenges in non-model crops through endogenous promoter optimization, and facilitate precise improvement of important traits in radish breeding programs.

Materials and methods

Identification of the *DMP* gene family in radish

The sequences of AtDMP proteins were retrieved from The Arabidopsis Information Resource (TAIR; www.arabidopsis.org)[30] and used as queries for BLASTP searches (*E*-value < 1×10^{-10}) against the NAU-LB chromosome-scale radish genome[31].

For domain identification and gene validation, Hidden Markov Model (HMM) profiles of the conserved DUF679 domain (Pfam ID: PF05078) were retrieved from the Pfam database (http://pfam-legacy.xfam.org)[32]. Candidate *DMP* genes were identified through a sequential screening workflow.

The physicochemical properties of RsDMP proteins, including molecular weight (Mw), theoretical isoelectric point (pI), the grand average of hydropathicity (GRAVY), and the aliphatic index were predicted using the ExPASy ProtParam tool (https://web.expasy.org/protparam)[33]. The subcellular localization of DMP proteins and the number of transmembrane domains were predicted using the DeepLoc tool (https://services.healthtech.dtu.dk/services/DeepLoc-2.0)[34] and the TMHMM tool (https://services.healthtech.dtu.dk/services/TMHMM-2.0)[35].

Analysis of chromosome localization and gene collinearity in radish

The chromosomal locations of *RsDMP* genes were mapped using the NAU-LB chromosome-scale radish genome[31]. Genomic coordinates were extracted from the annotated GFF3 file and visualized using TBtools to generate chromosome distribution maps[36].

To investigate evolutionary relationships, collinearity analysis was conducted among the genomes of *R. sativus*, *A. thaliana*, and *Brassica oleracea* using MCScanX, implemented within TBtools. Collinear gene pairs were visualized with TBtools, where connecting lines were used to highlight conserved genomic regions.

Analysis of the gene structure and conserved protein motifs

The conserved motifs of *RsDMP* genes were identified using the MEME (Multiple Expectation Maximization for Motif Elicitation) tool accessed via the MEME Suite website (https://meme-suite.org/meme/tools/meme)[37]. The analysis was conducted using MEME Suite version 5.4.1 with parameters set to the classic mode for motif discovery. The amino acid sequences of all analyzed conserved motifs identified in radish DMP proteins are provided in Supplementary Table S1. The structure of each *RsDMP* gene was analyzed using the Gene Structure Display Server (GSDS) (http://gsds.cbi.pku.edu.cn)[38]. Phylogenetic trees, along with gene structures, motifs, and conserved domains of radish and *Arabidopsis DMPs*, were generated using the TBtools software and the TVBOT tool (www.chiplot.online)[39].

Phylogenetic analysis of *DMP* genes

To investigate the phylogenetic relationships of *DMP* genes, protein sequences from 12 species—including *A. thaliana*, *R. sativus*, *Brassica juncea*, *Zea mays*, *Oryza sativa*, and *Medicago truncatula*—were aligned using ClustalW. A neighbor-joining phylogenetic tree was constructed in MEGA11[40] using the *p*-distance model with pairwise deletion and 1,000 bootstrap replicates. The resulting unrooted tree was visualized and annotated using the iTOL platform (https://itol.embl.de)[39]. Accession numbers for all the

DMP sequences were analyzed and are provided in Supplementary Table S2.

Analysis of promoter regions

The 2,000 bp upstream sequence of the initiation codon (ATG) for each gene was obtained from the NAU-LB database.[31] Then these sequences were submitted to the CARE (*Cis*-Acting Regulatory Element) search tool available in the PlantCARE database (https://bioinformatics.psb.ugent.be/webtools/plantcare/html) for the prediction and analysis of *cis*-acting regulatory elements, which were visualized using Tbtools. The distribution of *cis*-acting regulatory elements within the promoter regions is presented in Supplementary Table S3, followed by visualization using the TVBOT tool (www.chiplot.online)[39].

Transcriptome-based expression analysis

Transcriptomic data from four tissue types and various stress conditions were obtained from the Genomic Sequence Archive (GSA) database (https://bigd.big.ac.cn) under the biological engineering projects PRJCA011507, PRJNA606861, PRJNA598318, and PRJNA274183. The expression profiles of *RsDMP* genes were analyzed using $\log_2$-transformed fragments per kilobase of transcript per million mapped reads (FPKM) values, normalized to ensure comparability across samples. Detailed information is provided in Supplementary Table S4. Expression heat maps and hierarchical clustering were generated using TBtools, employing Euclidean distance matrices and complete linkage methods to illustrate expression divergence across developmental and reproductive tissues.

Quantitative real-time polymerase chain reaction (RT-qPCR) analysis

R. sativus NAU-LB seeds were germinated in the dark at room temperature for 2 d. After sprouting, they were transferred to a greenhouse for cultivation. Total RNA was extracted from the leaves, stems, flower buds, sepals, petals, pistils, and pollen, using the RNA simple Total RNA Kit (TIANGEN, Beijing, China). First-strand complementary DNA (cDNA) synthesis was performed with the HiScript II 1st Strand cDNA Synthesis Kit (Vazyme, Nanjing, China). Real-time quantitative polymerase chain reaction (RT-qPCR) was conducted using the LightCycler® 480 System (Roche, Mannheim, Germany). Relative expression levels were calculated using the $2^{-\Delta\Delta C_T}$ method[41], with *RsActin* as the internal control. Each reaction included three biological replicates and three technical replicates. The primers used for RT-qPCR are listed in Supplementary Table S5.

Subcellular localization of RsDMP9

The *RsDMP9* coding sequence was cloned into the plant expression vector pCAMBIA1300, with the empty vector (EV) serving as a negative control. Recombinant plasmids were then transformed into *Agrobacterium tumefaciens* GV3101 and cultured in LB medium containing 50 μg/mL kanamycin and 25 μg/mL rifampicin. When *Nicotiana benthamiana* plants reached the four to five-leaf stage, a suspension of *Agrobacterium* carrying 35S::*GFP*, RsDMP9-GFP, and the plasma membrane-specific marker PM-mCherry (OD_{600} = 0.8) was injected into the leaves using a syringe at a 1:1 ratio. After incubation in the dark for 48 h, GFP fluorescence was observed using a laser scanning confocal microscope (Zeiss, Baden-Württemberg, Germany). The primer sequences used for vector construction are listed in Supplementary Table S4.

Analysis of U6 promoter activity

A local BLAST search based on the AtU6-1 promoter was conducted in the *R. sativus* genome database[31]. Eight 1,500-bp *R. sativus* U6 snRNA promoters were identified and amplified by PCR using 2 × Hieff DNA Polymerase (Vazyme, Nanjing, China). The recombinant vector carrying the radish U6 promoter sequence and the plant expression vector pGreenII-0800-Luc were each subjected to double digestion. The target fragments were recovered and ligated using T4 ligase to construct expression vectors in which the luciferase reporter gene is driven by the radish U6 promoter. The constructed fusion expression vectors RsU6::*LUC*, AtU6-1::*LUC*, and the negative control pGreenII-0800-Luc were transformed into competent *A. tumefaciens* GV3101 cells. Finally, the transformed bacterial suspensions were infiltrated into the leaves of *N. benthamiana*. After incubation in the dark for 48 h, the leaves were collected and sprayed with 1 × D-luciferin potassium salt, incubated in the dark for 10 min, and then images of *in vivo* fluorescent signals were captured using a plant imaging system.

Isolation and transformation of radish protoplasts

Protoplasts were isolated from *R. sativus* NAU-LB seedlings and purified following a previously established protocol[42]. Healthy young leaves were excised and cut into 1 mm segments, which were then immersed in 20 mL of enzymatic hydrolysis solution (Supplementary Table S6). The plate was subsequently wrapped in tin foil and incubated on a shaker at 40 rpm at room temperature (RT). An equal volume of W5 solution (Supplementary Table S7) was added to the protoplast suspension, followed by centrifugation at 500 rpm for 10 min at 8 °C to separate intact protoplasts from the enzymatic mixture. The resulting protoplast pellet was resuspended in 2 mL of MMG solution (Supplementary Table S8). A 10 μL aliquot of the protoplast-MMG suspension was loaded onto a hemocytometer, where viability and concentration were assessed using an optical microscope. Finally, the protoplast concentration was adjusted to a range of 1.0×10^4 to 2.0×10^5 protoplasts/mL.

The transfection protocol was adapted from established methods used in *Brassicaceae* crops[43]. Briefly, 200 μL of the protoplast-MMG suspension was aliquoted into a 1.5-mL microcentrifuge tube, followed by the sequential addition of 10–15 μg of DNA and 215 μL of 40% PEG-calcium transfection solution (Supplementary Table S9), with gentle mixing using pipette tips. After incubation in the dark for 30 min at 25 °C, the reaction was terminated by adding an equal volume of W5. The mixture was centrifuged at 700 *g* using a benchtop centrifuge, followed by removal of the supernatant and resuspension in 500 μL of W5 solution. Transfected protoplasts were incubated in the dark at 25 °C for 36 h. Prior to imaging, the transformed protoplasts were homogenized by pipetting, pelleted by centrifugation at 700 *g* for 3 min, and the supernatant was discarded. Fluorescent signals were visualized using a laser scanning confocal microscope (LSM 800, Zeiss, Germany). All fluorescence observation experiments were repeated at least three times independently.

CRISPR-Cas9 gene-editing in radish protoplasts using the RsU6-6 promoter

To create the *pRsU6-6*::*GFP* vector, the promoter regions were amplified and inserted into the 2300GN-Cas9-EGFP vector. The RsU6-6 promoter fragments were amplified from genomic DNA using PCR and subsequently cloned into the *Sbf* I and *Sma* I sites of the 2300GN-Cas9-EGFP plasmid, respectively.

https://doi.org/10.48130/vegres-0026-0015

Genomic DNA was extracted from transfected radish protoplasts using the cetyltrimethylammonium bromide (CTAB) method[44]. Genomic fragments containing the target sites were amplified by PCR using DNA polymerase (Vazyme, Nanjing, China) and gene-specific primers. To detect mutations at the target sites, PCR products were subjected to high-throughput sequencing, and the sequencing data were analyzed using the CRISPResso2 tool[45]. Editing efficiency was calculated as the ratio of mutant DNA to total DNA. To detect mutation at each target site, triplicate amplicon sequencing was performed using genomic DNA. The PCR and sequencing primers used in the study are listed in Supplementary Table S5.

Statistical analysis

All data are presented as the mean ± standard deviation (SD) using at least three biological replicates. SPSS Statistics version 22.0 (SPSS Institute Inc., Chicago, IL, USA) was used for the statistical analysis.

Results

Identification and phylogenetic analysis of the *DMP* gene family

To analyze phylogenetic relationships within the *DMP* family, an unrooted phylogenetic tree was constructed using 173 DMP proteins from both monocot and dicot crop species (Fig. 1). The DMP proteins cluster into five major clades. Clade I consists of 17 DMP protein homologs, except for AtDMP10. No other homologous proteins from dicot plants are found in this clade. Clade II includes 24 DMPs, which contain the male gametophyte-specific genes *AtDMP8* and *AtDMP9*. Multiple homologs of *AtDMP8* and *AtDMP9* in the *Brassicaceae* may have originated from multiple genome-wide duplications and triploidization events during the genome evolution of the *Brassicaceae* ancestors. Based on these findings, these genes may share conserved functions and thus represent potential candidate genes for HI in *R. sativus*. Clade III contains 40 direct homologs of AtDMP1 and AtDMP2, which are considered senescence-related proteins. These proteins are involved in remodeling the endoplasmic reticulum and vacuolar membranes. Clade IV consists of 26 DMPs, with *R. sativus* homologs RsDMP3 and RsDMP5 corresponding to AtDMP3 and AtDMP5 in *A. thaliana*, respectively. The largest clade, Clade V, contains 66 DMPs, including RsDMP6-like, RsDMP6, RsDMP4-like, RsDMP4, and RsDMP7. These data indicate diverse functional roles of DMP proteins in plant aging, membrane remodeling, and HI.

Based on the NAU-LB radish genome database, 13 *RsDMP* genes containing the DMP domain were identified at the genome-wide level. A combination of similarity and diversity was observed in several key physicochemical properties of the RsDMP proteins, including length, molecular weight (Mw), theoretical isoelectric point (pI), the aliphatic index, and hydropathicity (Supplementary Table S10). The predicted lengths of the RsDMP polypeptides range from 185 to 242 amino acids, with a molecular weight varying from 20.34 kDa (RsDMP2) to 26.38 kDa (RsDMP9). The aliphatic index ranges from 84.55 (RsDMP9) to 97.53 (RsDMP4-like). The theoretical pI ranges from 5.12 (RsDMP6) to 9.03 (RsDMP7), suggesting that most RsDMP proteins are relatively stable. Predictions of transmembrane domains and subcellular localization revealed that most RsDMP proteins contain two to five transmembrane domains, with potential localization in the lysosome, while six are likely localized to the cell membrane. These findings indicate that the DMP family of proteins shares conserved transmembrane domains.

Chromosomal localization and collinearity analysis of *RsDMP* genes

Chromosomal localization analysis revealed that *RsDMP* genes are distributed across six chromosomes (Fig. 2a). Notably, *RsDMP6* and *RsDMP6-like* exhibit tandem duplication on chromosome 4, while *RsDMP2* and *RsDMP2-like* are tandem duplicates on chromosome 5, suggesting that these genes may have arisen from whole-genome duplication (WGD) events during radish evolution. Collinearity analysis identified 19 collinear blocks between *R. sativus* and *B. oleracea*, but only four blocks between radish and *A. thaliana* (Fig. 2b). This indicates significantly lower synteny between *R. sativus* and *Arabidopsis*, likely reflecting divergent adaptation strategies or evolutionary trajectories. In contrast, the stronger collinearity between the radish and the cabbage suggests a conserved genomic organization of this gene family, which may reflect their closer evolutionary relationship.

Analysis of RsDMP structure and conserved protein motifs in radish

To investigate the diversity and similarity of gene structures and motifs between proteins from these two species, a phylogenetic tree was constructed using MEGA11 (Fig. 3a). The MEME server was employed to predict ten distinct conserved motifs in DMP proteins, revealing that all DMP proteins contain three to seven conserved motifs (Fig. 3b). Although most DMP proteins exhibit both similar and divergent conserved sites, motifs 1, 2, 3, 4, and 5 constitute the majority of conserved regions in RsDMP proteins, suggesting that these active sites are critical for the transmembrane functions of the proteins. Except for *AtDMP7* and *RsDMP7*, all other *DMP* genes consist of a single exon (Fig. 3c). This finding underscores the highly conserved gene structure within the *DMP* family, suggesting a potential evolutionary significance of this single-exon configuration in maintaining functional integrity.

Cis-element analysis of *DMP* promoters in radish

The prediction of *cis*-acting elements in the upstream 2,000 bp of the *DMP* gene family in *R. sativus* revealed the presence of various environmental and stress-responsive elements (Fig. 4a). The promoters of 13 *RsDMP* genes contain 40 growth and development-related elements, 170 light-responsive elements, 158 phyhormone-responsive elements, and 224 stress-related responsive elements. The highest number of binding sites was detected in the promoters of *RsDMP1-like* and *RsDMP6-like* (56 binding sites each), followed by *RsDMP2* (54 binding sites). In contrast, the promoter of *RsDMP4* contains the fewest binding sites (32 binding sites). The greater abundance of stress-responsive elements in these promoters suggests that their expression is linked to stress response and regulation. Among the growth and stress-responsive elements, dehydration-responsive elements (containing MYB and MYC transcription factor binding sites), anaerobic response elements (ARE), and the W box (fungal elicitor-responsive) are predominant (Fig. 4b). In addition, there are the light-responsive *cis*-elements in the *RsDMP* promoters, including G-box, Box 4, TCT-motif, GT1-motif, MRE, and AE-box, indicating that the expression of *RsDMP* genes may be regulated by light. Furthermore, hormonal-responsive elements such as abscisic acid response (ABRE), TGACG-motif (methyl jasmonate

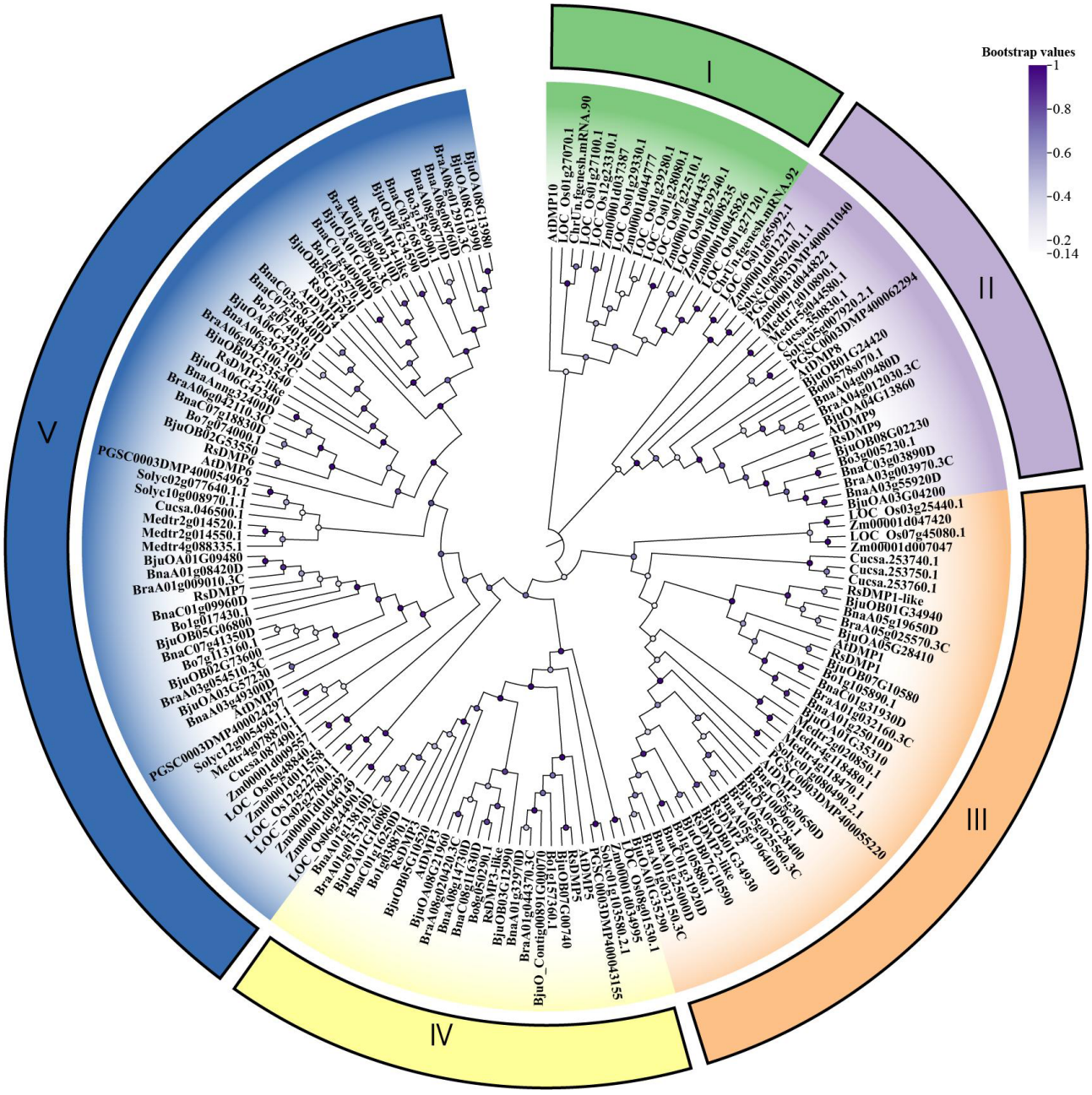

Fig. 1 Phylogenetic relationships of DMP among 12 plant species. The DMP protein were divided into five clades, represented by colors. Bootstrap values are shown on the nodes. For accession ID details of the genes, refer to Supplementary Table S10.

[MeJA] response), CGTCA-motif (MeJA response), and TCA-element (salicylic acid response), among others, indicate that *RsDMP* genes are primarily regulated by abscisic acid, MeJA, and salicylic acid signaling pathways. These results reveal that *RsDMP* genes are involved in hormone response, stress response, and other plant growth processes (Fig. 4b).

Expression profiles of the *RsDMP* family in different tissues and abiotic stress

To investigate the functional roles of the *RsDMP* family in radish, the expression profiles of 13 *RsDMP* genes across different tissues were analyzed using existing transcriptomic data (Fig. 5a). *RsDMP2-like* exhibited the highest expression level in leaf tissues. *RsDMP9*, *RsDMP2-like*, and *RsDMP1* showed differential expression in stamens, with *RsDMP9* displaying the highest expression.

To explore the potential functions of *RsDMP* genes under abiotic stress, transcriptomic data for 13 *RsDMP* genes were analyzed under heavy metal stress (chromium [Cr], lead [Pb], and cadmium [Cd]), salt stress, and heat stress (Fig. 5b). *RsDMP4* was downregulated under both Cr and heat stress, while *RsDMP2* and *RsDMP7* were downregulated under all three heavy metals and heat stress. Similarly, *RsDMP6-like* exhibited downregulation under heavy metal and heat stresses. In contrast, *RsDMP3* was upregulated to varying degrees under all three heavy metals. *RsDMP3-like* also showed upregulation under Pb stress, suggesting that *RsDMP3* and *RsDMP3-like* may participate in detoxification, defense, or repair mechanisms, potentially contributing to abiotic stress tolerance.

https://doi.org/10.48130/vegres-0026-0015

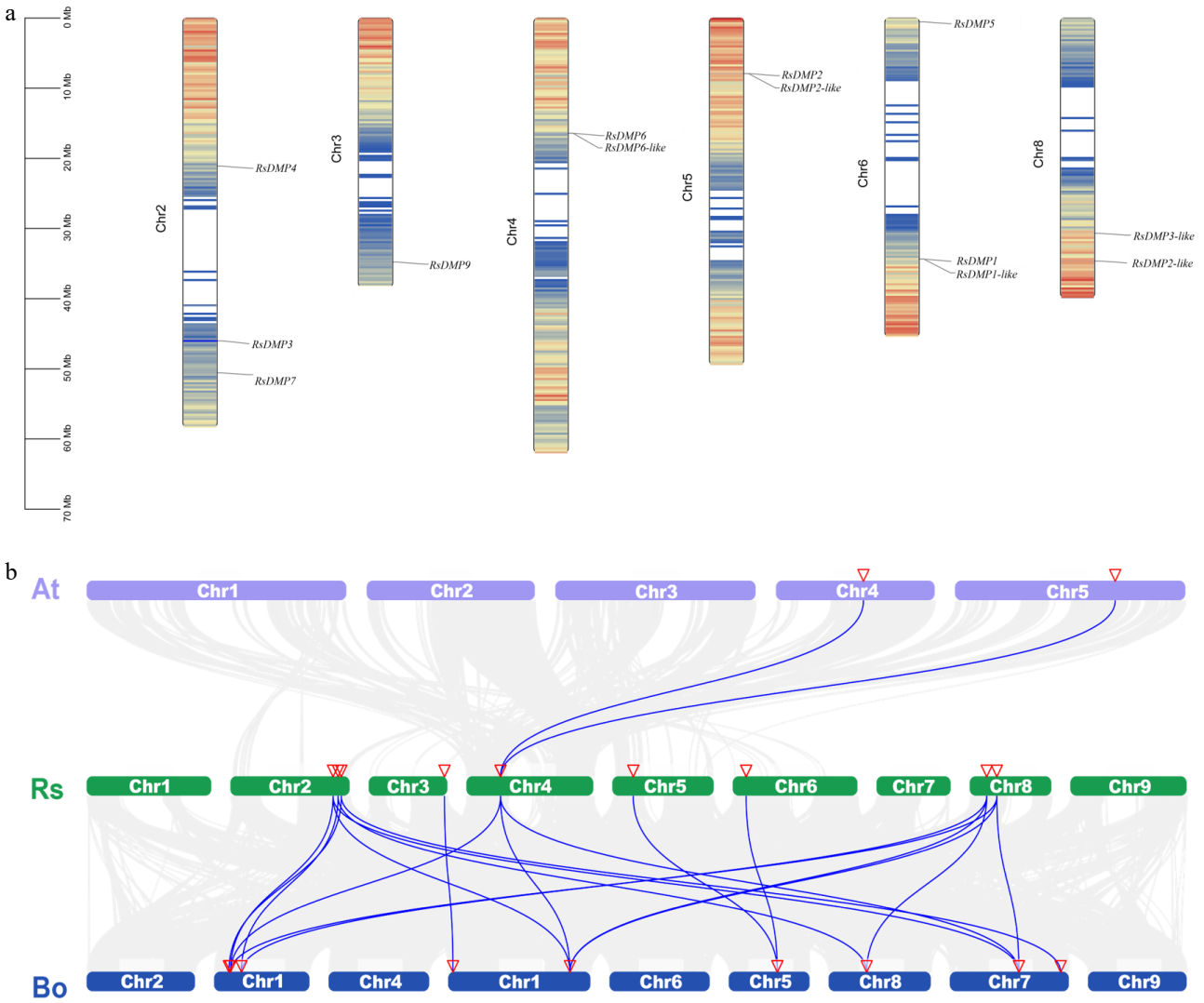

Fig. 2 Chromosomal locations and collinearity of *DMP* genes. (a) *DMP* chromosome mapping. The *DMP* genes of radish were distributed on six chromosomes. Mb, megabase. (b) Collinearity analysis among *Raphanus sativus* (Rs), *Arabidopsis thaliana* (At), and *Brassica oleracea* (Bo). Blue lines indicate collinear gene pairs.

RT-qPCR analysis of *RsDMP* genes and subcellular localization

To further investigate the expression patterns of *RsDMP* genes in reproductive organs, RT-qPCR was performed on 13 *RsDMP* genes across six radish tissues: sepals, pollen, petals, pistils, taproots, and leaves (Fig. 6). Compared to non-reproductive tissues (taproots and leaves), *RsDMP* genes generally exhibited higher expression in reproductive organs. *RsDMP4* and *RsDMP6* were highly expressed in pistils, suggesting potential roles in double fertilization or ovule development. *RsDMP2-like*, *RsDMP3-like*, *RsDMP5*, and *RsDMP9* showed predominant expression in pollen. The elevated expression of *RsDMP9* is consistent with its *Arabidopsis* homologs *AtDMP8/AtDMP9*, which regulate double fertilization. *RsDMP1* and *RsDMP2* displayed varying degrees of upregulation in petals, potentially linked to floral morphogenesis. *RsDMP1-like*, *RsDMP4-like*, *RsDMP6-like*, and *RsDMP7* were most highly expressed in sepals, indicating their involvement in sepal development. Collectively, these tissue-specific expression patterns highlight the potential roles of *RsDMP* genes in reproductive processes and underscore their functional diversity in radish.

To further explore the functional basis of these tissue-specific expression patterns, particular focus was placed on *RsDMP9*, whose predominant expression in pollen and homology to *AtDMP8/AtDMP9* (known regulators of double fertilization) strongly suggest a conserved role in reproductive processes, including a predicted HI function. Prior research has shown that DMP HI proteins perform their functions at the plasma membrane. To determine the subcellular localization of RsDMP9, an RsDMP9-GFP fusion construct was transiently expressed in *N. benthamiana* leaves via *Agrobacterium*-mediated infiltration. Imaging revealed precise colocalization of the RsDMP9-GFP fluorescence signal with the plasma membrane-specific marker PM-mCherry (Supplementary Fig. S1), demonstrating that RsDMP9 localizes to the plasma membrane. This spatial distribution pattern is consistent with its predicted role as a membrane-associated transporter protein.

Cloning and transcriptional activity analysis of endogenous U6 promoters in radish

Based on the radish genome and homology alignment, eight highly homologous U6 small nuclear RNA (snRNA) loci were

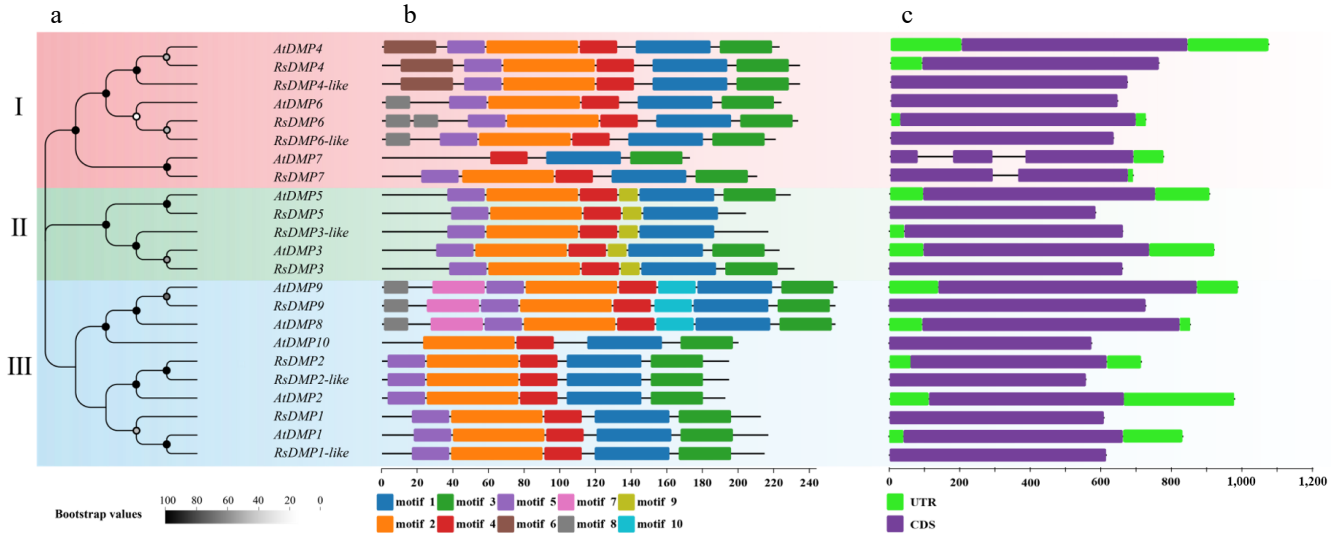

Fig. 3 Gene structure and motif distribution of *RsDMP* and *AtDMP* genes. (a) Constructing phylogenetic trees of *RsDMP* genes and *AtDMP* genes using MEGA 11 based on the NJ method. (b) Schematic diagram of the conserved motifs of RsDMP and AtDMP proteins. The motifs 1 to 10 are highlighted with different colored boxes. For the details of each motif, refer to Supplementary Table S2. (c) Distribution of structure for each *RsDMP* and *AtDMP* gene. The purple boxes represent CDS, the green boxes indicate an untranslated region, and the black line represents introns.

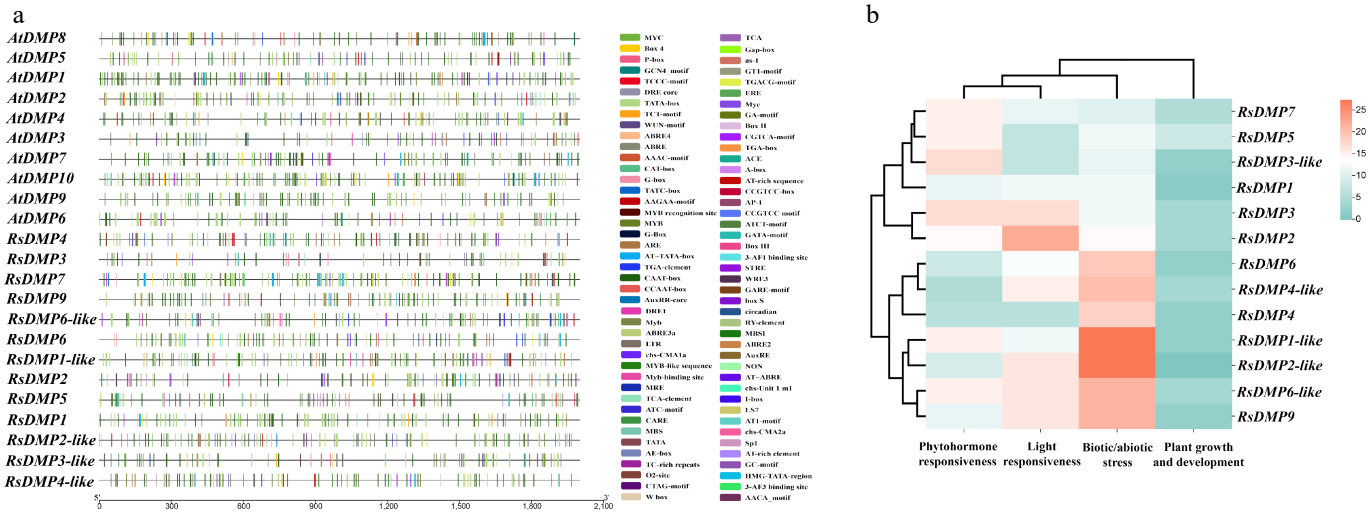

Fig. 4 Characterization of *cis*-regulatory elements (CAREs) in the promoter regions of *RsDMP* genes. (a) Distribution of CAREs in different colored rectangles. (b) Variation in different types of *cis*-acting regulatory elements (CAREs, refer to Supplementary Table S3).

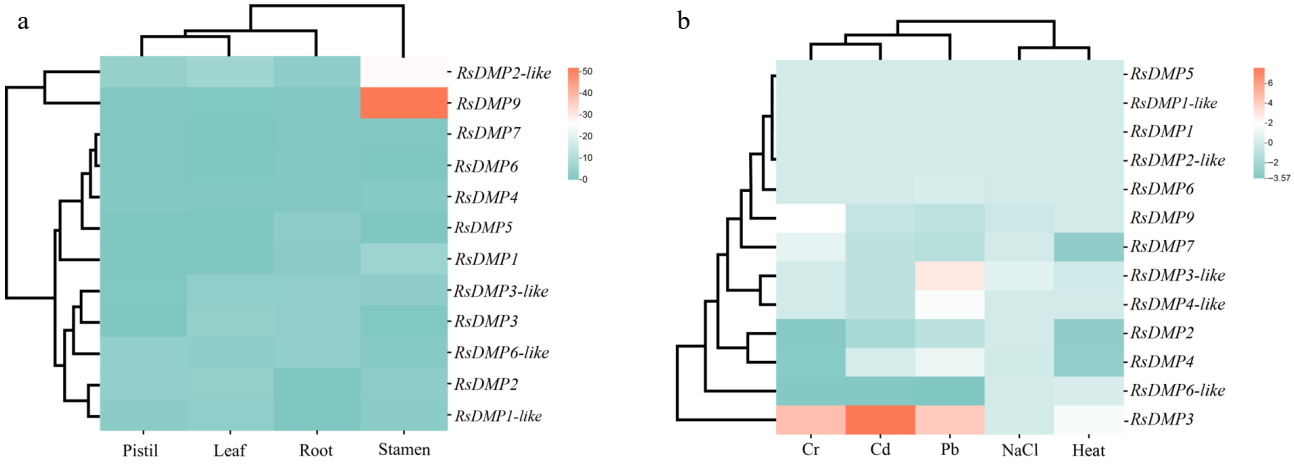

Fig. 5 Expression pattern of radish *DMP* genes. (a) Transcriptome-based expression profiling of *RsDMP* genes from four radish tissues consisted of leaf, root, pistil, and stamen. (b) The relative expression of *RsDMP* genes under Cd stress (200 μM/24 h), Cr stress (200 μM/24 h), heat stress (42 °C/24 h), Pb stress(200 μM/24 h), and NaCl stress (200 mM/24 h). Cd, cadmium; Cr, chromium; and Pb, lead. The plant material is sourced from NAU-LB. For details of each gene expression, refer to Supplementary Table S4.

https://doi.org/10.48130/vegres-0026-0015

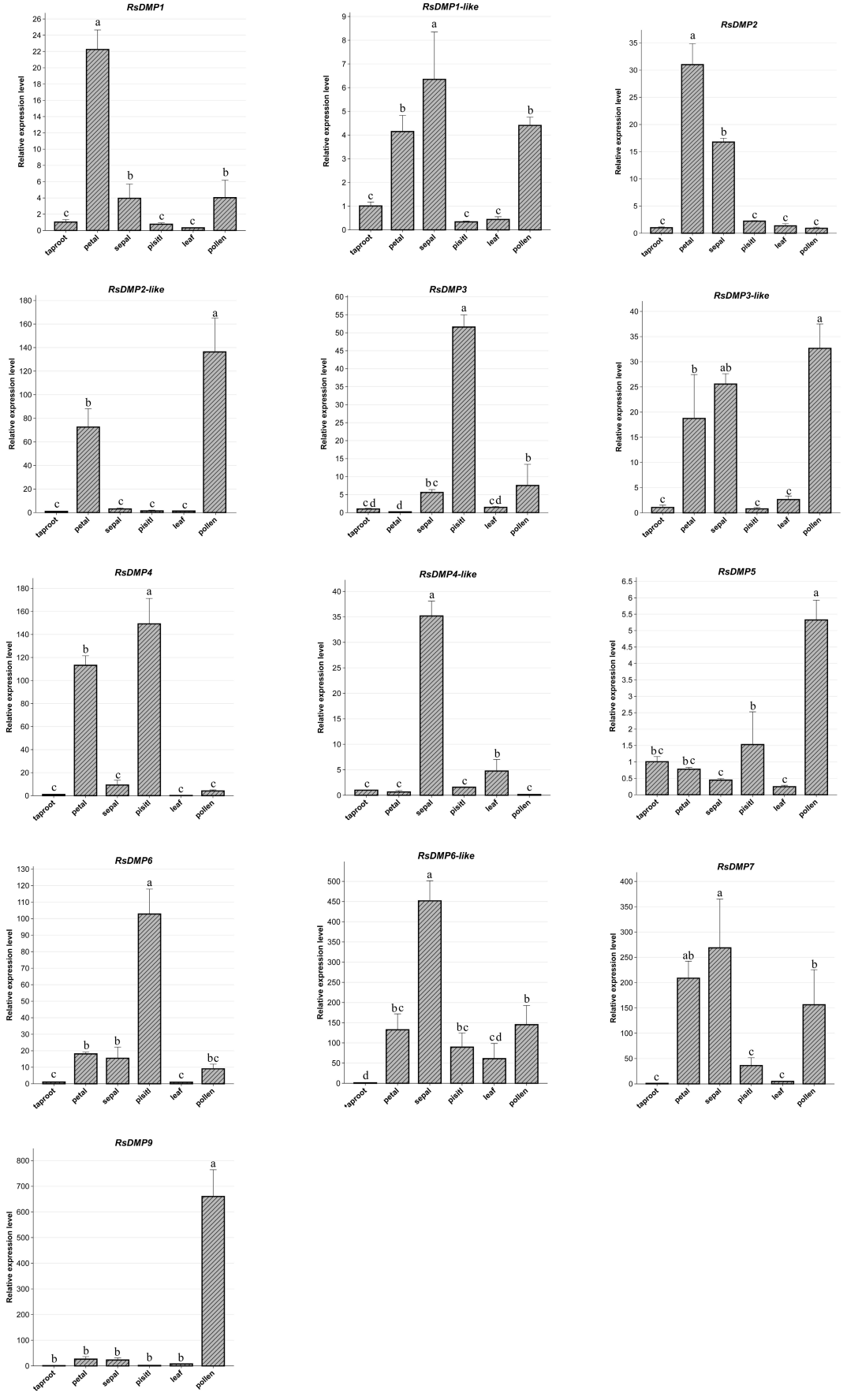

Fig. 6 The relative expression levels of *RsDMP* genes in different tissues by qPCR analysis. Data are shown as the means ± SD from three biological replicates. Different letters above the bar indicate a significant differences among columns by Duncan's multiple comparison test ($p < 0.05$).

identified. Correspondingly, eight upstream promoter fragments—designated RsU6-1, RsU6-2, RsU6-4, RsU6-6, RsU6-8, RsU6-9, RsU6-10, and RsU6-13—were successfully cloned from radish genomic DNA. Sequence alignment revealed that all eight RsU6 promoters, along with the *Arabidopsis* AtU6-1 promoter, initiate transcription at a conserved guanine (G) nucleotide and contain canonical core regulatory elements: a TATA box located about 30 bp upstream of the transcription start site (TSS) and an upstream sequence element (USE) approximately 60 bp upstream (Fig. 7a).

To assess transcriptional activity, these eight RsU6 promoters and AtU6-1 (the positive control) were cloned into the pGreen II 0800-Luc vector and transiently transformed into *N. benthamiana* leaves via *Agrobacterium* infiltration. Fluorescence signal analysis indicated that RsU6-6 and AtU6-1 drove the strongest luciferase expression, followed by RsU6-8, RsU6-10, RsU6-9, and RsU6-4. In contrast, RsU6-1, RsU6-2, RsU6-13, and EV showed extremely weak luciferase signals, indicating marked heterogeneity in transcriptional activity across the RsU6 promoter family. Notably, RsU6-6 not only outperformed most RsU6 promoters but also exhibited stronger luciferase expression than AtU6-1, highlighting its superior transcriptional potency as an endogenous promoter candidate in radish (Fig. 7b).

Truncation of U6 promoters could reduce the length of the sgRNA expression cassette and enhance transcriptional activity by removing redundant sequences while preserving key regulatory elements (Fig. 7d). To assess the effect of truncation on RsU6-6 activity, a truncated 326-bp variant of RsU6-6 was cloned into pGreen II 0800-Luc. Fluorescence signal analysis showed that the truncated RsU6-6 promoter exhibited higher luciferase activity than AtU6-1 (Fig. 7c), confirming that truncation did not reduce its transcriptional activity.

CRISPR-Cas9 gene-editing in radish protoplasts using the RsU6-6 promoter

Functional validation of the HI gene *RsDMP9* (*Rsa3g028070*), an ortholog of *AtDMP8/AtDMP9*, was performed using CRISPR/Cas9-mediated genome editing. Two sgRNAs targeting *RsDMP9* were designed using web-based tools. To compare the efficiency of the RsU6-6 and AtU6-1 promoters in driving sgRNA expression in radish protoplasts, a CRISPR/Cas9 vector containing two sgRNA expression cassettes was constructed. Specifically, sgRNA1 and sgRNA2 were driven by the RsU6-6 and AtU6-1 promoters, respectively, and co-cloned into the gene-editing vector 2300GN-Cas9-EGFP (Fig. 8a, c). After incubation for 48 h, GFP fluorescence in protoplasts was detected via confocal microscopy (Supplementary Fig. S2). The transfection efficiency of radish protoplasts was 43.1% ± 3.1% (Fig. 8b). Subsequently, protoplast DNA was extracted, and sequences containing the two target sites of gRNA1 and gRNA2 were amplified. Next-generation sequencing (NGS) data analyzed using CRISPResso2 revealed that the mutation frequency induced by gRNA1 driven by RsU6-6 was 6.69% (99 mutant reads) (Fig. 8d, e). Among these mutations, the frameshift mutation rate caused by a 1-base deletion located 3 bp upstream of the PAM sequence was 0.88% (21 reads), consistent with the typical Cas9 cleavage site. In contrast, the mutation frequency of sgRNA2 driven by AtU6-1 was significantly lower at 0.55% (26 reads), with no detectable frameshift mutations, indicating lower editing efficiency (Supplementary Fig. S3).

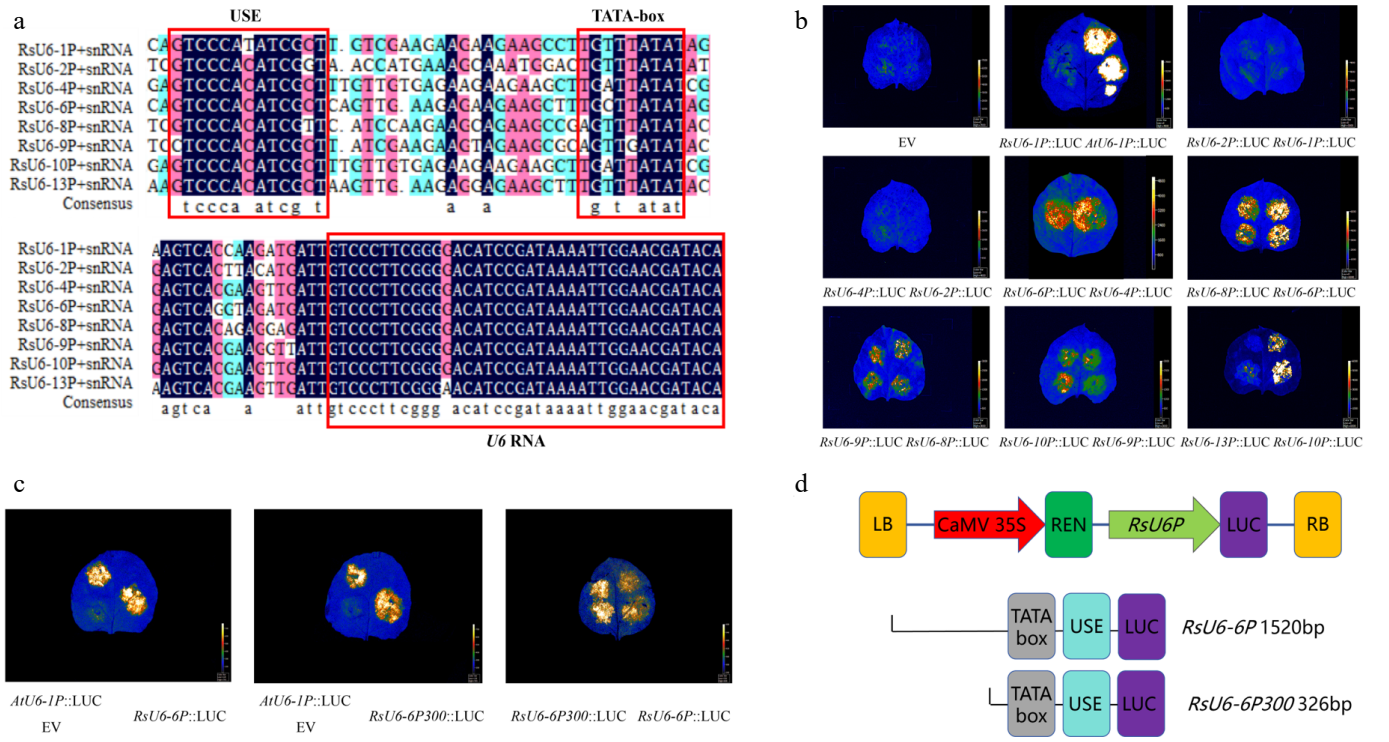

Fig. 7 Functional analysis and expression vector validation of the RsU6 promoter. (a) Conservation element analysis of the RsU6 promoter region (including sequence alignment of TATA box, USE, and U6 RNA-related conserved sequences). (b) RsU6P::*LUC* and AtU6-1P::*LUC* are transiently expressed in *N. benthamiana* leaves. (c) RsU6P-6P300::*LUC*, RsU6P-6P::*LUC*, and AtU6-1P::*LUC* are transiently expressed in *N. benthamiana* leaves. (d) Schematic diagram of the RsU6P-6P300::*LUC* and RsU6P-6P::*LUC* constructs, along with a comparative diagram of the functional segments between the truncated variant and the full-length sequence.

https://doi.org/10.48130/vegres-0026-0015

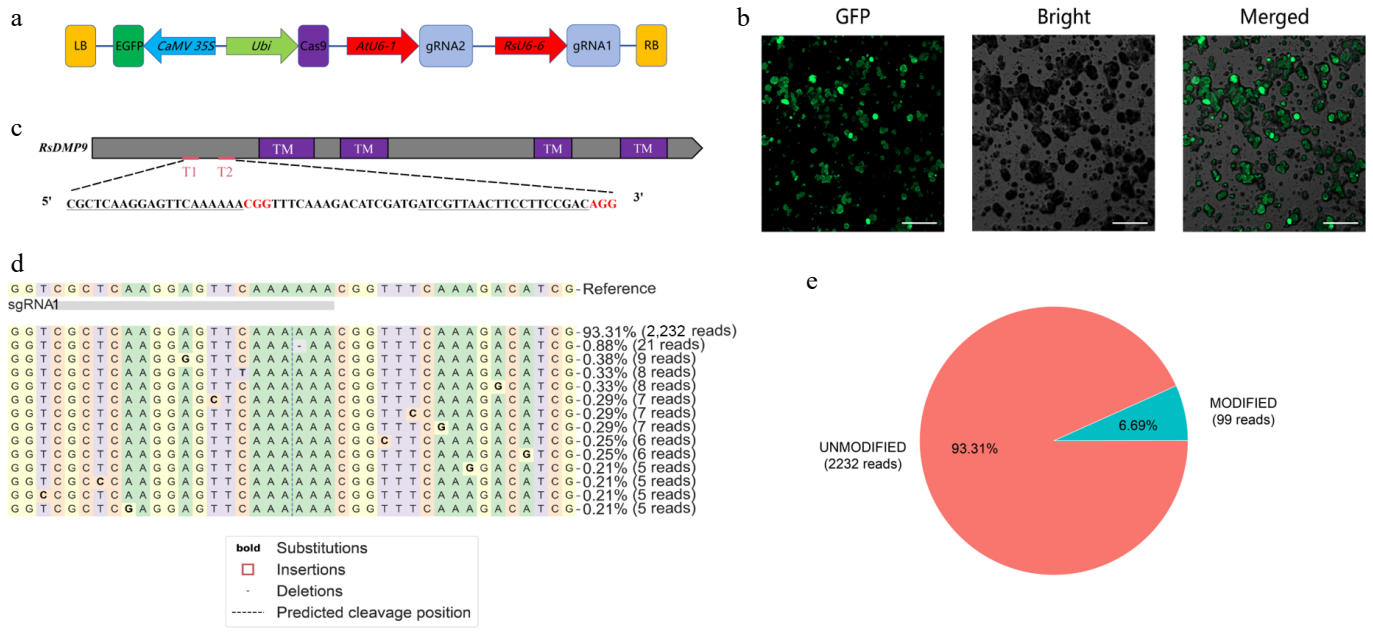

Fig. 8 The radish protoplast transient transfection system was employed to validate the activity of CRISPR/Cas9 vectors. (a) Schematic diagram of the CRISPR/Cas9 construct targeting *RsDMP9*. EGFP, enhanced green fluorescent protein. (b) Radish protoplasts were imaged under GFP, bright field, and merged channel. Green fluorescent signals reflected the transformed cells. Scale bar = 100 μm. (c) Schematic of *RsDMP9*. Grey blocks, gene coding region; purple blocks, predicted transmembrane domains (TMs); black lines, the region (T1 and T2) targeted by sgRNAs. (d) The types of mutations detected in the sgRNA1 target site. (e) Pie chart showing the mutation as a percentage of total reads.

Discussion

Characterization and evolutionary dynamics of *RsDMP* genes

This study presents the first genome-wide identification of the *DMP* gene family in radish. There are ten *DMP* genes in *A. thaliana*[10], while a total of 13 *RsDMP* genes were identified in radish, the same number as in the closely related species *B. oleracea*. Phylogenetic analysis revealed that these genes could be divided into five clades and exhibited high homology with *DMP* genes from *A. thaliana*, *B. juncea*, *B. oleracea*, and *B. napus*. *RsDMP9* clustered in subclade II alongside the pollen-specific genes *AtDMP8*/*AtDMP9*, indicating functional conservation in reproductive processes. Notably, Brassicaceae species typically possess two to four orthologs of AtDMP8/AtDMP9, whereas radish retains only one. This is most likely because the Brassicaceae ancestor underwent multiple whole-genome duplication (WGD) events. However, during the subsequent rediploidization process, redundant gene copies were gradually eliminated through unequal crossing-over during homologous recombination or chromosomal fragment deletion[21]. Intriguingly, *RsDMP2* and *RsDMP2-like* (tandem duplicates on chromosome 5), *RsDMP6* and *RsDMP6-like* (tandem duplicates on chromosome 6) indicate lineage-specific gene duplication events in radish. Cross-species collinearity analysis demonstrated stronger synteny between radish and *B. oleracea DMP* genes compared to *Arabidopsis DMP* genes, reflecting convergence and adaptive similarity during *Brassicaceae* evolution.

Tissue-specific expression of *RsDMP* genes and its multifunctional role in plant reproduction and stress adaptation

The DMP family represents a class of membrane proteins found exclusively in green plants. Members of this family participate in various physiological processes, particularly senescence and reproduction[11,12,46]. In this study, tissue-specific transcriptome analysis and RT-qPCR data demonstrated that *RsDMP* genes are predominantly expressed in reproductive organs (e.g., stamens, pistils, and pollen) compared to vegetative organs such as taproots and leaves.

With the development of haploid breeding technology, DMP family proteins have garnered increasing attention and are widely used in HI across various species, including maize[17], *Arabidopsis*[10], potato[21], tomato[47], watermelon[19], and cucumber[20]. In this study, *RsDMP9* exhibited the highest expression level in pollen. Consistent with previous studies suggesting that *DMP* genes are involved in HI, this indicates that it may be a male gamete-specific gene[10]. Subcellular localization experiments confirmed that RsDMP9 is localized to the plasma membrane. These results align with its orthologs, maize ZmDMP and *Arabidopsis* AtDMP8/AtDMP9, which are associated with sperm-egg fusion and fertilization[11,46]. It can be inferred that RsDMP9 regulates fertilization through gamete membrane interactions[10,16].

The elevated expression of *RsDMP1-like*, *RsDMP4-like*, *RsDMP6-like*, and *RsDMP7* in sepals highlights their roles in sepal development. These tissue-specific expression patterns emphasize the functional diversification of *DMP* genes in reproductive processes, providing new opportunities to investigate their pleiotropic functions. Additionally, *RsDMP3* expression was upregulated under heavy metal stress, along with the abundance of stress-responsive *cis*-elements in their promoters, suggesting that *DMP* genes may integrate developmental and environmental signals.

In vitro editing of *RsDMP9* in radish protoplasts

HI-edit technology, which combines haploid inducer lines with CRISPR/Cas9-mediated gene editing, represents a recent advancement in HI. This approach utilizes *in vitro* HI to produce haploid plants within two generations, significantly improving crop breeding efficiency. Prior research has shown that targeted editing of

genes such as *DMP*, *CENH3*, and *MTL*/*PLA1*/*NLD* can induce haploid plant formation[5,17,48]. Among these, the *DMP* gene has been the most widely applied across various crops for HI. These findings highlight the considerable potential of gene-specific editing for HI, offering valuable applications for accelerating crop improvement.

Protoplasts serve as an ideal system for genetic manipulation due to their ability to directly take up exogenous DNA, proteins, or chemicals. The protoplast transformation system was first established in *Arabidopsis*. Recently, a protoplast-based transient gene expression system for genome editing was established in citrus[28]. In this study, a radish protoplast transient transformation system successfully validated the editing activity of CRISPR/Cas9 vectors targeting *RsDMP9*, confirming that radish protoplasts provide a reliable platform for rapid assessment of editing efficiency. Next-generation sequencing data revealed a 6.69% mutation frequency at the T1 site in protoplasts, including 0.88% frameshift mutations, demonstrating the feasibility of applying this CRISPR/Cas9 editing system to stable transformation in radish. These findings lay a critical foundation for the future development of an HI system targeting *RsDMP9* in radish. However, there was relatively low overall editing efficiency in radish compared to the established protoplast editing systems in other plant species. For example, in citrus, an optimized PEG-mediated method for callus protoplasts achieved a gene mutation frequency of 14.2%, more than twice that of the radish system[28]. Similarly, in the medicinal plant *Salvia miltiorrhiza*, the selection of endogenous regulatory elements and a codon-optimized Cas9 driven by the SlEF1α promoter significantly boosted editing efficiency, demonstrating that selection of tailored genetic elements can effectively enhance CRISPR/Cas9 performance in protoplasts[49]. Despite these limitations, the successful validation of CRISPR/Cas9 activity in radish protoplasts confirms its potential as a rapid platform for assessing editing efficiency. Future work should focus on optimizing transfection protocols, exploring endogenous regulatory elements suitable for radish, and testing alternative Cas nucleases. These improvements will enhance the utility of the radish protoplast system, providing a more robust foundation for developing HI systems and advancing genome-editing applications in radish genetic improvement.

The critical role of U6 promoters in CRISPR/Cas9-mediated genome editing

A total of eight highly homologous U6 snRNA loci were identified in radish. Sequence alignment revealed conserved structural features shared with functionally validated U6 promoters from *Arabidopsis* (AtU6-1). All RsU6 promoters initiate transcription at a conserved G nucleotide, consistent with the canonical transcription start site (TSS) of U6 promoters[50]. Critical core elements were identified: a TATA box located approximately 30 bp upstream of the TSS and an Upstream Sequence Element (USE) about 60 bp upstream (Fig. 7a), both of which are essential for Pol III recruitment and transcriptional initiation[50]. These conserved elements strongly suggest that RsU6 promoters are functional Pol III promoters, providing a foundation for their application in sgRNA expression.

RsU6-6 and AtU6-1 (positive control) exhibited the strongest luciferase activity, followed by RsU6-8, while the remaining RsU6 promoters (RsU6-8, RsU6-10, RsU6-9, RsU6-4, RsU6-1, RsU6-2, and RsU6-13) displayed lower but detectable activity.

A major challenge in CRISPR vector construction is the large size of full-length U6 promoters, which can limit cloning efficiency and the design of sgRNA expression cassettes. Truncation of U6 promoters, while retaining core regulatory elements, has been shown to shorten the cassette length and even enhance activity by removing redundant or inhibitory sequences[25]. In apple (*Malus domestica*) and cotton (*Gossypium barbadense*), truncation of MdU6-10P (from 1,500 to 275 bp) and GbU6-5P could enhance transcriptional activity[25,51]. To optimize RsU6-6 for practical use, it was truncated to 326 bp. Strikingly, the truncated RsU6-6 promoter exhibited higher luciferase activity than AtU6-1 (Fig. 7c), indicating that key regulatory elements are preserved within this 326-bp region. The truncated RsU6-6 thus represents a superior tool for radish genome editing: Its reduced size simplifies vector construction, while its high activity ensures robust sgRNA expression.

Our study presents the characterization of endogenous U6 promoters in radish, identifying RsU6-6 (both the full-length and truncated forms) as a leading candidate for sgRNA expression. Its high activity, conserved regulatory elements, and compact truncated form (326 bp) make it ideal for developing efficient CRISPR/Cas9 systems in radish. Additionally, RsU6-6, exhibiting moderate activity, could serve as a secondary promoter for multiplex editing, enabling the co-expression of multiple sgRNAs without promoter crosstalk.

Ultimately, these endogenous U6 promoters will accelerate precision breeding in radish, enabling targeted improvements in agronomic traits such as haploid breeding, storage quality, and nutritional content.

Conclusions

In total, 13 *DMP* genes were identified in the radish genome. Phylogenetic analysis indicated that *RsDMP9* clusters alongside haploid-inducing genes from *A. thaliana*. These genes are distributed across six chromosomes and exhibit tandem duplication events. Collinearity analysis revealed greater similarity to *B. oleracea* than to *A. thaliana*. RsDMP proteins display conserved structural features. Promoter analysis identified regulatory elements responsive to light, growth regulators, hormones, and stress. Transcriptomic and RT-qPCR data demonstrated predominant expression in reproductive tissues; notably, *RsDMP9* showed significantly higher expression in pollen. Subcellular localization confirmed that RsDMP9 is localized to the plasma membrane.

Radish endogenous U6 promoters were further characterized, and RsU6-6 (a 326-bp truncated variant) was prioritized for robust sgRNA expression. By integrating RsU6-6-driven CRISPR/Cas9 with protoplast transient editing, a 6.69% mutation frequency (0.88% frameshift mutations) for *RsDMP9* in radish protoplasts was achieved.

This protoplast-based editing system could be efficiently validate gene functions and enhance the precision of key trait improvements in radish breeding programs.

Author contributions

The authors confirm their contributions to the paper as follows: study conception and design: Liu L, Zhang P, Zhao B, Dong H, Ying J; data collection: Zhang P, Zhao B, Dong H, Wang M; analysis and interpretation of results: Zhang P, Zhao B, Cui F, Li J; draft manuscript preparation: Zhang P, Zhao B, Liu L, Li J, Zhang X, Xu L, Wang Y, Chen S. All authors reviewed the results and approved the final version of the manuscript.

Data availability

The datasets generated during and/or analyzed in the current study are available from the corresponding author on reasonable request.

Acknowledgments

This study was supported by the Key Technology R&D Program of Jiangsu Province (Grant No. BE2023366), Jiangsu Seed Industry Revitalization Project (Grant No. JBGS[2021]071), the Jiangsu Agricultural S&T Innovation Fund (Grant No. CX[2023]1013), National Natural Science Foundation of China (Grant No. 32573040), Yancheng S&T Key Project (Grant No. YCBN202312), Postgraduate Research & Practice Innovation Program of Jiangsu Province (Grant No. KYCX19_0562) and the Project Funded by the Priority Academic Program Development of Jiangsu Higher Education Institutions (PAPD).

Conflict of interest

The authors declare that they have no conflict of interest.

Supplementary information accompanies this paper online at: https://doi.org/10.48130/vegres-0026-0015.

Dates

Received 21 December 2025; Revised 16 April 2026; Accepted 27 April 2026; Published online 14 July 2026

References

[1] Gamba M, Asllanaj E, Raguindin PF, Glisic M, Franco OH, et al. 2021. Nutritional and phytochemical characterization of radish (*Raphanus sativus*): a systematic review. *Trends in Food Science & Technology* 113:205–218

[2] Singh BK. 2021. Radish (*Raphanus sativus* L.): breeding for higher yield, better quality and wider adaptability. In *Advances in Plant Breeding Strategies: Vegetable Crops*, eds. Al-Khayri JM, Jain SM, Johnson DV. Cham: Springer International Publishing. pp. 275–304 doi: 10.1007/978-3-030-66965-2_7

[3] Ferrie AMR, Caswell KL. 2011. Isolated microspore culture techniques and recent progress for haploid and doubled haploid plant production. *Plant Cell, Tissue and Organ Culture (PCTOC)* 104:301–309

[4] Shi C, Zhao Z, Zhong Y, Qiao Y, Zhang L, et al. 2025. Reprogramming of microspore fate via *BBM-BAR1* for highly efficient *in vivo* haploid induction. *Cell* 188:6109–6120.e15

[5] Kelliher T, Starr D, Richbourg L, Chintamanani S, Delzer B, et al. 2017. MATRILINEAL, a sperm-specific phospholipase, triggers maize haploid induction. *Nature* 542:105–109

[6] Li Y, Lin Z, Yue Y, Zhao H, Fei X, et al. 2021. Loss-of-function alleles of *ZmPLD3* cause haploid induction in maize. *Nature Plants* 7:1579–1588

[7] Gilles LM, Khaled A, Laffaire JB, Chaignon S, Gendrot G, et al. 2017. Loss of pollen - specific phospholipase NOT LIKE DAD triggers gynogenesis in maize. *The EMBO Journal* 36:707–717

[8] Kelliher T, Starr D, Wang W, McCuiston J, Zhong H, et al. 2016. Maternal haploids are preferentially induced by *CENH3-tailswap* transgenic complementation in maize. *Frontiers in Plant Science* 7:414

[9] Wang N, Gent JI, Dawe RK. 2021. Haploid induction by a maize *cenh3* null mutant. *Science Advances* 7:eabe2299

[10] Zhong Y, Chen B, Li M, Wang D, Jiao Y, et al. 2020. A *DMP*-triggered in vivo maternal haploid induction system in the dicotyledonous *Arabidopsis*. *Nature Plants* 6:466–472

[11] Cyprys P, Lindemeier M, Sprunck S. 2019. Gamete fusion is facilitated by two sperm cell-expressed DUF679 membrane proteins. *Nature Plants* 5:253–257

[12] Kasaras A, Kunze R. 2010. Expression, localisation and phylogeny of a novel family of plant-specific membrane proteins. *Plant Biology* 12:140–152

[13] Kasaras A, Kunze R. 2017. Dual-targeting of *Arabidopsis* DMP1 isoforms to the tonoplast and the plasma membrane. *PLoS One* 12:e0174062

[14] van der Graaff E, Schwacke R, Schneider A, Desimone M, Flügge UI, et al. 2006. Transcription analysis of *Arabidopsis* membrane transporters and hormone pathways during developmental and induced leaf senescence. *Plant Physiology* 141:776–792

[15] Nawade B, Bosamia TC, Lee JH, Jang JH, Lee OR. 2023. Genome-wide characterization of the soybean DOMAIN OF UNKNOWN FUNCTION 679 membrane protein gene family highlights their potential involvement in growth and stress response. *Frontiers in Plant Science* 14:1216082

[16] Sprunck S. 2020. Twice the fun, double the trouble: gamete interactions in flowering plants. *Current Opinion in Plant Biology* 53:106–116

[17] Zhong Y, Liu C, Qi X, Jiao Y, Wang D, et al. 2019. Mutation of *ZmDMP* enhances haploid induction in maize. *Nature Plants* 5:575–580

[18] Pan Z, Li Z, Han Y, Sun J. 2024. Genome-wide identification and expression analysis of the *DMP* and *MTL* genes in sweetpotato (*Ipomoea batatas* L.). *Genes* 15:354

[19] Tian S, Zhang J, Zhao H, Zong M, Li M, et al. 2023. Production of double haploid watermelon via maternal haploid induction. *Plant Biotechnology Journal* 21:1308–1310

[20] Yin S, Li S, Sun L, Shi K, Fan S, et al. 2024. Mutating the maternal haploid inducer gene *CsDMP* in cucumber produces haploids *in planta*. *Plant Physiology* 194:1282–1285

[21] Zhang J, Yin J, Luo J, Tang D, Zhu X, et al. 2022. Construction of homozygous diploid potato through maternal haploid induction. *aBIOTECH* 3:163–168

[22] Li Y, Li D, Xiao Q, Wang H, Wen J, et al. 2022. An *in planta* haploid induction system in *Brassica napus*. *Journal of Integrative Plant Biology* 64:1140–1144

[23] Chen L, Wang S, Zhang YH, Li J, Xing ZH, et al. 2017. Identify key sequence features to improve CRISPR sgRNA efficacy. *IEEE Access* 5:26582–26590

[24] Preece R, Georgiadis C, Gkazi SA, Etuk A, Christi A, et al. 2020. 'Mini'U6 Pol III promoter exhibits nucleosome redundancy and supports multiplexed coupling of CRISPR/Cas9 effects. *Gene Therapy* 27:451–458

[25] Long L, Guo DD, Gao W, Yang WW, Hou LP, et al. 2018. Optimization of CRISPR/Cas9 genome editing in cotton by improved sgRNA expression. *Plant Methods* 14:85

[26] Charrier A, Vergne E, Dousset N, Richer A, Petiteau A, et al. 2019. Efficient targeted mutagenesis in apple and first time edition of pear using the CRISPR-Cas9 system. *Frontiers in Plant Science* 10:40

[27] Zhou J, Wang G, Liu Z. 2018. Efficient genome editing of wild strawberry genes, vector development and validation. *Plant Biotechnology Journal* 16:1868–1877

[28] Yang W, Ren J, Liu W, Liu D, Xie K, et al. 2023. An efficient transient gene expression system for protein subcellular localization assay and genome editing in citrus protoplasts. *Horticultural Plant Journal* 9:425–436

[29] Wang Y, Zhang YA, Dong Y, Li D, Shi S, et al. 2022. A highly efficient mesophyll protoplast isolation and PEG-mediated transient expression system in eggplant. *Scientia Horticulturae* 304:111303

[30] Reiser L, Bakker E, Subramaniam S, Chen X, Sawant S, et al. 2024. The *Arabidopsis* information resource in 2024. *Genetics* 227:iyae027

[31] Xu L, Wang Y, Dong J, Zhang W, Tang M, et al. 2023. A chromosome-level genome assembly of radish (*Raphanus sativus* L.) reveals insights into genome adaptation and differential bolting regulation. *Plant Biotechnology Journal* 21:990–1004

[32] Bateman A, Coin L, Durbin R, Finn RD, Hollich V, et al. 2004. The Pfam protein families database. *Nucleic Acids Research* 32:D138–D141

[33] Gasteiger E, Hoogland C, Gattiker A, Duvaud S, Wilkins MR, et al. 2005. Protein identification and analysis tools on the ExPASy server. In *The Proteomics Protocols Handbook*, ed. Walker JM. Totowa, NJ: Humana Press. pp. 571–607 doi: 10.1385/1-59259-890-0:571

[34] Thumuluri V, Almagro Armenteros JJ, Johansen AR, Nielsen H, Winther O. 2022. DeepLoc 2.0: multi-label subcellular localization prediction using protein language models. *Nucleic Acids Research* 50:W228–W234

[35] Hallgren J, Tsirigos KD, Pedersen MD, Almagro Armenteros JJ, Marcatili P, et al. 2022. DeepTMHMM predicts alpha and beta transmembrane proteins using deep neural networks. *bioRxiv* 1–12

[36] Chen C, Chen H, Zhang Y, Thomas HR, Frank MH, et al. 2020. TBtools: an integrative toolkit developed for interactive analyses of big biological data. *Molecular Plant* 13:1194–1202

[37] Bailey TL, Williams N, Misleh C, Li WW. 2006. MEME: discovering and analyzing DNA and protein sequence motifs. *Nucleic Acids Research* 34:W369–W373

[38] Hu B, Jin J, Guo AY, Zhang H, Luo J, et al. 2015. GSDS 2.0: an upgraded gene feature visualization server. *Bioinformatics* 31:1296–1297

[39] Xie J, Chen Y, Cai G, Cai R, Hu Z, et al. 2023. Tree Visualization By One Table (tvBOT): a web application for visualizing, modifying and annotating phylogenetic trees. *Nucleic Acids Research* 51:W587–W592

[40] Tamura K, Stecher G, Kumar S. 2021. MEGA11: molecular evolutionary genetics analysis version 11. *Molecular Biology and Evolution* 38:3022–3027

[41] Livak KJ, Schmittgen TD. 2001. Analysis of relative gene expression data using real-time quantitative PCR and the $2^{-\Delta\Delta C_T}$ method. *Methods* 25:402–408

[42] Yoo SD, Cho YH, Sheen J. 2007. *Arabidopsis* mesophyll protoplasts: a versatile cell system for transient gene expression analysis. *Nature Protocols* 2:1565–1572

[43] Yu X, Yu J, Lu Y, Li W, Huo G, et al. 2024. An efficient and universal protoplast-based transient gene expression system for genome editing in *Brassica* crops. *Horticultural Plant Journal* 10:983–994

[44] Porebski S, Bailey LG, Baum BR. 1997. Modification of a CTAB DNA extraction protocol for plants containing high polysaccharide and polyphenol components. *Plant Molecular Biology Reporter* 15:8–15

[45] Clement K, Rees H, Canver MC, Gehrke JM, Farouni R, et al. 2019. Accurate and rapid analysis of genome editing data from nucleases and base editors with CRISPResso2. *Nature Biotechnology* 37:224–226

[46] Li L, Hou S, Xiang W, Song Z, Wang Y, et al. 2022. The egg cell is preferentially fertilized in *Arabidopsis* double fertilization. *Journal of Integrative Plant Biology* 64:2039–2046

[47] Zhong Y, Chen B, Wang D, Zhu X, Li M, et al. 2022. *In vivo* maternal haploid induction in tomato. *Plant Biotechnology Journal* 20:250–252

[48] Liu C, Li X, Meng D, Zhong Y, Chen C et al. 2017. A 4-bp insertion at *ZmPLA1* encoding a putative phospholipase a generates haploid induction in maize. *Molecular Plant* 10:520–522

[49] Shao J, Peng B, Zhang Y, Yan X, Yao X, et al. 2024. A high-efficient protoplast transient system for screening gene editing elements in *Salvia miltiorrhiza*. *Plant Cell Reports* 43:45

[50] Li F, Xue M, Guo D, Zhu L, Li Y, et al. 2025. A truncated endogenous U6 promoter enables high-efficiency CRISPR editing in flax (*Linum usitatissimum* L.). *Plants* 14:1142

[51] Bian S, Han X, Yuan G, Zhang L, Tian Y, et al. 2019. Cloning and functional analysis of U6 promoter in apple. *Scientia Agricultura Sinica.* 52:4364–4373 (in Chinese)